Research Article | Vol. 25, No. 9 | 1 May 2017 | OPTICS EXPRESS 9511

Optics EXPRESS

Design of square-shaped beam homogenizer for petawatt-class Ti:sapphire amplifier

SEUNGJIN HWANG,[1] TAESHIN KIM,[1] JONGMIN LEE,[2] AND TAE JUN YU[1,2,*]

[1]*Department of Advanced Green Energy and Environment, Handong Global University, Pohang 37554, South Korea*

[2]*Global Institute of Laser Technology, Global Green Research and Development Center, Handong Global University, Pohang 37554, South Korea*

[*]*taejunyu@handong.edu*

Abstract: We have designed a square-shaped beam homogenizer using a lens array for pumping a petawatt-class Ti:sapphire amplifier. The designed beam homogenizer generated a flat-top uniform square pump beam with 5.1% of edge steepness and 2.7% of RMS spatial uniformity, respectively. This pump beam generated an output beam with 74 J of energy and 56.8% of extraction efficiency, respectively. A scalar diffraction and two-dimensional amplification simulation were performed for optimization. The results indicate the possibility of improving an amplification efficiency and developing a compact square petawatt-class laser system.

OCIS codes: (140.3300) Laser beam shaping; (140.3280) Laser amplifiers.

References and links

1. H. Kiriyama, M. Mori, A. S. Pirozhkov, K. Ogura, A. Sagisaka, A. Kon, T. Z. Esirkepov, Y. Hayashi, H. Kotaki, M. Kanasaki, H. Sakaki, Y. Fukuda, J. Koga, M. Nishiuchi, M. Kando, S. V. Bulanov, K. Kondo, P. R. Bolton, O. Slezak, D. Vojna, M. Sawicka-Chyla, V. Jambunathan, A. Lucianetti, and T. Mocek, "High-contrast, high- intensity petawatt-class laser and applications," IEEE J. Sel. Top. Quantum Electron. **21**(1), 232–249 (2015).
2. H. Kiriyama, T. Shinomura, M. Mori, Y. Nakai, M. Tanoue, S. Kondo, S. Kanazawa, A. S. Pirozhkov, T. Z. Esirkepov, Y. Hayashi, K. Ogura, H. Kotaki, M. Suzuki, I. Daito, H. Okada, A. Kosuge, Y. Fukuda, M. Nishiuchi, M. Kando, S. V. Bulanov, K. Nagashima, M. Yamagiwa, K. Kondo, A. Sugiyama, P. R. Bolton, S. Matsuoka, and H. Kan, "Ultra-Intense, High Spatio-Temporal Quality Petawatt-Class Laser System and Applications," Appl. Sci. **3**, 214–250 (2013).
3. S. Fujioka, Y. Arikawa, S. Kojima, T. Johzaki, H. Nagatomo, H. Sawada, S. H. Lee, T. Shiroto, N. Ohnishi, A. Morace, X. Vaisseau, S. Sakata, Y. Abe, K. Matsuo, K. F. F. Law, S. Tosaki, A. Yogo, K. Shigemori, Y. Hironaka, Z. Zhang, A. Sunahara, T. Ozaki, H. Sakagami, K. Mima, Y. Fujimoto, K. Yamanoi, T. Norimatsu, S. Tokita, Y. Nakata, J. Kawanaka, T. Jitsuno, N. Miyanaga, M. Nakai, H. Nishimura, H. Shiraga, K. Kondo, M. Bailly-Grandvaux, C. Bellei, J. Jorge Santos, and H. Azechi, "Fast ignition realization experiment with high-contrast kilo-joule peta-watt LFEX laser and strong external magnetic field," Phys. Plasmas **23**, 056308 (2016).
4. L. Willingale, S. P. D. Mangles, S. R. Nagel, C. Bellei, A. E. Dangor, M. C. Kaluza, C. Kamberidis, S. Kneip, Z. Najmudin, P. M. Nilson, A. G. R. Thomas, and K. Krushelnick, "Proton acceleration from near critical density foam targets using the Vulcan Petawatt laser," CLF Annual Report 2005/2006, 61–63 (2005).
5. S. Kawata, T. Izumiyama, T. Nagashima, M. Takano, D. Barada, Q. Kong, Y. J. Gu, P. X. Wang, Y. Y. Ma, and W. M. Wang, "Laser ion acceleration toward future ion beam cancer therapy–Numerical simulation study," Laser Ther. **22**(2), 103–114 (2013).
6. W. P. Leemans, A. J. Gonsalves, H. S. Mao, K. Nakamura, C. Benedetti, C. B. Schroeder, C. Tóth, J. Daniels, D. E. Mittelberger, S. S. Bulanov, J. L. Vay, C. G. R. Geddes, and E. Esarey, "Multi-GeV Electron Beams from Capillary-Discharge-Guided Subpetawatt Laser Pulses in the Self-Trapping Regime," Phys. Rev. Lett. **113**, 245002 (2014).
7. N. Savege, "Germans Plan Petawatt Laser to Zap Brain Tumors," http://spectrum.ieee.org/the-human-os/biomedical/devices/giant-german-laser-will-zap-brain-tumors-one-day.
8. V. V. Lozhkarev, G. I. Freidman, V. N. Ginzburg, E. V. Katin, E. A. Khazanov, A. V. Kirsanov, G. A. Luchinin, A. N. Malshakov, M. A. Martyanov, O. V. Palashov, A. K. Poteomkin, A. M. Sergeev, A. A. Shaykin, and I. V. Yakovlev, "Compact 0.56 Petawatt laser system based on optical parametric chirped pulse amplification in KD*P crystals," Laser Phys. Lett. **4**(6), 421–427 (2007).
9. https://www.thalesgroup.com/en/
10. http://www.amplitude-technologies.com/

#287193 https://doi.org/10.1364/OE.25.009511
Journal © 2017 Received 21 Feb 2017; revised 10 Apr 2017; accepted 12 Apr 2017; published 17 Apr 2017

Optics EXPRESS

11. O. Novák, H. Turčičová, M. Smrž, J. Huynh, M. Pfeifer, P. Straka, "Broadband femtosecond OPCPA system driven by the single-shot narrow-band iodine photodissociation laser SOFIA," Appl. Phys. B **108**, 501-508 (2012).
12. F. Canova, O. Uteza, J-P. Chambaret, M. Flury, S. Tonchev, R. Fechner, and O. Parriaux, "High-efficiency, broad band, high-damage threshold high-index gratings for femtosecond pulse compression," Opt. Express **15**(23), 15324–15334 (2007).
13. S. Banerjee, P. D. Mason, K. Ertel, P. J. Phillips, M. D. Vido, O. Chekhlov, M. Divoky, J. Pilar, J. Smith, T. Butcher, A. Lintern, S. Tomlinson, W. Shaikh, C. Hooker, A. Lucianetti, C. Hernandez-Gomez, T. Mocek, C. Edwards, and J. L. Collier, "100 J-level nanosecond pulsed diode pumped solid state laser," Opt. Lett. **41**(9), 2089–2092 (2016).
14. M. Tanaka, H. Kiriyama, Y. Ochi, Y. Nakai, H. Sasao, H. Okada, H. Daido, P. Bolton, and S. Kawanishi, "High-energy, spatially flat-top green pump laser by beam homogenization for petawatt scale Ti:sapphire laser systems," Opt. Commun. **282**, 4401-4403 (2009).
15. K. Fuse, "Flattop beam generation and multibeam processing using aspheric and diffractive optics," J. Laser Micro. Nanoen. **5**(2), 156–162 (2010).
16. R. Voelkel, and K. J. Weible, "Laser beam homogenizing: limitations and constraints," Proc. SPIE 7102, 71020J (2008).
17. K. Ertel, C. Hooker, S. J. Hawkes, B. T. Parry, and J. L. Collier, "ASE suppression in a high energy Titanium sapphire amplifier," Opt. Express **16**(11), 8039–8049 (2008).
18. F. Ple, M. Pittman, G. Jamelot, and J-P. Chambaret, "Design and demonstration of a high-energy booster amplifier for a high-repetition rate petawatt class laser system," Opt. Lett. **32**(3), 238–240 (2007).
19. S. Banerjee, K. Ertel, P. D. Mason, P. J. Phillips, M. D. Vido, J. M. Smith, T. J. Butcher, C. Hernandez-Gomez, R. J. S. Greenhalgh, and J. L. Collier, "DiPOLE: a 10 J, 10 Hz cryogenic gas cooled multi-slab nanosecond Yb:YAG laser," Opt. Express **23**(15), 19542–19551 (2015).
20. T. J. Yu, S. K. Lee, J. H. Sung, J. W. Yoon, T. M. Jeong, and J. Lee, "Generation of high-contrast, 30 fs, 1.5 PW laser pulses from chirped-pulse amplification Ti:sapphire laser," Opt. Express **20**(10), 10807–10815 (2012).
21. M. Zimmermann, N. Lindlein, R. Voelkel, and K. J. Weible, "Microlens laser beam homogenizer: from theory to application," Proc. SPIE 6663, 666302 (2007).
22. D. Voelz, Computational Fourier Optics : A MATLAB Tutorial (SPIE Press, 2011).
23. Y. Chu, X. Liang, L. Yu, Y. Xu, L. Xi, L. Ma, X. Lu, Y. Liu, Y. Leng, R. Li, and Z. Xu, "High-contrast 2.0 Petawatt Ti:sapphire laser system," Opt. Express **21**(24), 29231–29239, (2013).
24. ISO 13694:2015, Optics and Optical Instruments - Lasers and Laser Related Equipment - Test Method for Laser Beam Power (Energy) Density Distribution, (2015).
25. S. Bollanti, P. D. Lazzaro, and D. Murra, "Performance of a zoom homogenizer for reshaping coherent laser beams," Opt. Commun. **264**, 174–179 (2006).
26. Y. Jin, A. Hassan, and Y. Jiang, "Freeform microlens array homogenizer for excimer laser beam shaping," Opt. Express **24**(22), 24846–24858 (2016).
27. L. M. Frantz, and J. S. Nodvik, "Theory of Pulse Propagation in a Laser Amplifier," J. Appl. Phys. **34**, 2346–2349 (1963).
28. G. Cheriaux, P. Rousseau, F. Salim, J. P. Chambaret, B. Walker, and L. F. Dimauro, "Aberration-free stretcher design for ultrashort-pulse amplification," Opt. Lett. **21**(6), 414–416 (1996).
29. W. Koechner, *Solid-state Laser Engineering* (Springer, 2006).

1. Introduction

The generation of an ultra-intense laser pulse using chirped-pulse amplification (CPA) has been used in research fields such as compact laser acceleration, medical applications, nuclear power, and radiation applications [1–3]. Research into the applications mentioned above was only accessible in approved facilities, but the development of a table-top-scale ultra-intense laser system has made it possible for the basic science to be extended into industrial applications [4–6].

There has been renewed interest in developing a compact petawatt-class CPA laser system in recent years [7–10]. Several studies have been conducted on reducing the size of the laser system by utilizing optical parametric chirped pulse amplification (OPCPA) [11], enhancing the damage threshold of optical components such as the mirror and diffraction grating [12], and shaping a square beam [13]. The OPCPA technique has been commonly used in front-end systems [11]. A high damage threshold of the optical components enables the use of small optical components while the same energy is transferred. A square-shaped pump beam was used in the main amplifier to generate a square-shaped amplified beam [13]. In this article, we will concentrate only on the method for shaping a square beam owing to the following:

Optics EXPRESS

The utilization of a square beam makes the laser system compact. A square beam can reduce the size of the optical components by 11% compared with those of a circular beam with the same fluence. In addition, a square beam can require 27% more area than a circular beam. This makes it possible to reduce the risk of the damage to the optical component and to make the pulse compressor and optical components compact.

A square-shaped laser beam can be created by pumping a gain medium with a square pump beam. The pump beam is required to have a high steepness for efficient amplification [1, 14]. If the steepness is low, the pump energy remains in the medium owing to a poor gain of the edge, which has a low pumping fluence. The spatial uniformity of the pump beam is also an important characteristic. The spatial distribution of the output beam follows the spatial distribution of the pump beam owing to the high gain of the amplifier [14]. Therefore, it is important to make the pump beam to have a high steepness and uniform spatial distribution.

The diffraction optical element (DOE) and the lens array can generate a square uniform beam [15, 16]. The DOE has been used to create a uniform beam having a high steepness, but there was a loss of energy [15]. A beam homogenizer using a lens array is more suitable for high-energy pumping because there is theoretically no loss of energy, and the incident beam profile does not significantly affect the performance. Some studies proposed methods utilizing a DOE or lens array to homogenize a pump beam for a petawatt-class laser system [17, 18]. However, a circular beam was used to pump the gain medium, not a square beam. A previous study of a square pump beam in a high-power laser examined a 100-J-level laser that used Yb:YAG slabs pumping with laser diodes [19]. It was difficult to find other studies that used a square pump beam in a high-power laser system.

In this paper, we designed a beam homogenizer using two lens arrays to convert several nonuniform circular beams into a uniform square beam. For a numerical simulation, the final booster amplifier was designed for tens of joules of output energy. An input beam with 2.4 J of energy was amplified into a square beam with more than 74 J of energy through this three-pass amplifier. A 2D amplification simulation was performed to optimize a beam homogenizer.

2. Beam homogenizer for square flat-top beam

2.1. Beam homogenizer

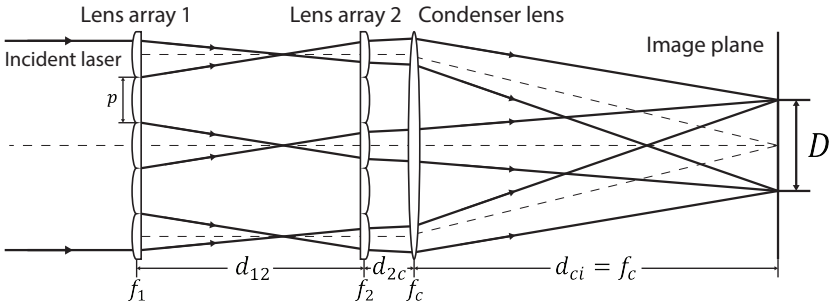

Fig. 1. Schematic of beam homogenizer for pumping Ti:sapphire gain medium.

To make a uniform square beam into a Ti:sapphire gain medium, the beam homogenizer consists of two lens arrays and one condenser lens, as shown in Fig. 1 [16]. The incident beam is a square arrangement of four nonuniform beams of 25-mm diameter and 30-mm spacing. The first lens array (LA1) divides the incident beam into several square beamlets. These beamlets overlap on the image plane and form a uniform square beam. The size of the square beam on the

Optics EXPRESS

image plane is expressed by Eq. (1) [16]:

$$D = \frac{pf_c}{f_1 f_2}(f_1 + f_2 - d_{12}), \tag{1}$$

For the image condition($d_{12} = f_2$), the size of the square beam on the image plane is simplified to Eq. (2) [16].

$$D = p\frac{f_c}{f_2}, \tag{2}$$

The size of the square beam (D) can be defined by three parameters: the pitch size of the lens array (p), the focal length (f_2) of the second lens array (LA2), and the focal length (f_c) of the condenser lens (L_c). The beam homogenizer must maintain its distance from the image plane owing to the structure of the petawatt amplifier [20]. In consideration of this, f_c is fixed at 3 m. The amplifier setup fixes the beam size. Therefore, the characteristics of the beam homogenizer can be simply described by one variable, p.

The size of the pump beam with 126 J of energy is fixed at 6 cm for 3.3 J/cm^2 of pumping fluence. The Ti:sapphire crystal used in this study has a thickness of 25 mm, and its absorption coefficient is 1.2 cm^{-1}. With this property, an energy of 120 J is stored in the crystal with 95% of absorption. The lens pitch varies from 0.5 to 6 mm. d_{2c} is set arbitrarily to avoid damage to LA2 because it does not affect the size of the pump beam, as shown in Eq. (2). We assume that the interval (d_{2c}) between LA2 and L_c is close to zero in the simulation. d_{2c} does not affect the diffraction effect or the size of the pump beam, but it does affect the divergence of the output beam [21].

2.2. Numerical analysis process

Figure 2 shows the propagation simulation process and the image of each plane. The entire propagation process consists of two propagations: the first interval is between the input beam and LA2, and the second interval is between L_c and a center of the Ti:sapphire, as shown in Fig. 2. The simulation parameters are listed in Table 1.

Table 1. Simulation parameters of beam homogenizer

p [mm]	f_1 [mm]	f_2=d_{12}[mm]	d_{2c} [mm]	f_c=d_{ci}[m]
0.5	15	25		
1.0	30	50		
2.0	60	100		
3.0	90	150	0	3.0
4.0	120	200		
5.0	150	250		
6.0	180	300		

The Fourier convolution theorem [22] in Eqs. (4) or (6) can be used for the first propagation from the input beam to the LA2 plane. h and t_{LA1} are an impulse response and a transmittance function of LA1. F, F^{-1}, and n are the Fourier transformation, the inverse Fourier transformation, and the number of lens elements in the lens array, respectively. x_n and y_n are the coordinates based on the each lens element in the lens array. Equation (4) can calculate the image of the short propagation distance without aliasing errors, and can use the memory efficiently. However, its computational cost is very high owing to many calculations of the Fourier transformation. Equation (6) requires only one calculation of the Fourier transform, but it requires a long

Optics EXPRESS

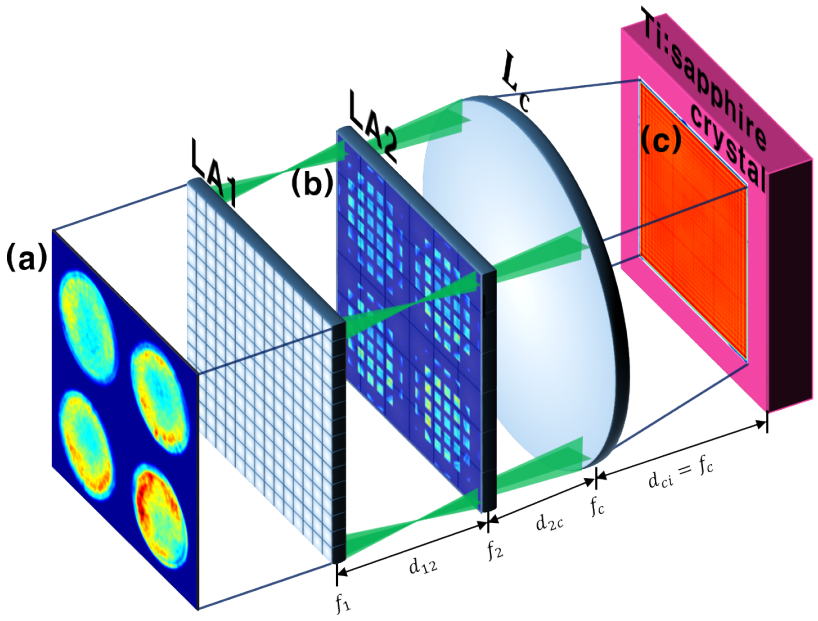

Fig. 2. Propagation simulation process: (a) intensity of input beam $|E_{in}(x,y)|^2$, (b) intensity on LA2 plane $|E_{LA2}(x,y)|^2$, and (c) intensity of output beam $|E_{crystal}(x,y)|^2$.

propagation distance or more memory than Eq. (4). Δx_n and Δy_n are the space shifts between the center of the beam homogenizer and the center of the lens elements in the lens array.

$$h(x,y,z) = \frac{exp(jkz)}{j\lambda z} exp\Big[\frac{jk}{2z}(x^2+y^2)\Big], \tag{3}$$

Case (i): propagation of each lenslet

$$E_{LA2}(x,y) = \sum_n F^{-1}\{E_{in}(x_n,y_n)t_{LA_1}(x_n,y_n)F\{h(x_n,y_n,d_{12})\}\}, \tag{4}$$

$$t_{LA1}(x,y) = exp\Big[-j\frac{k}{2f_1}(x^2+y^2)\Big], \tag{5}$$

Case (ii): propagation of an entire beam

$$E_{LA2}(x,y) = F^{-1}\{F\{E_{in}(x,y)t_{LA1}(x,y)\}F\{h(x,y,d_{12})\}\}, \tag{6}$$

$$t_{LA1}(x,y) = \sum_n \Big[rect\Big(\frac{x-\Delta x_n}{p}\Big)rect\Big(\frac{y-\Delta y_n}{p}\Big)exp\Big[-j\frac{k}{2f_1}\{(x-\Delta x_n)^2+(y-\Delta y_n)^2\}\Big]\Big], \tag{7}$$

To calculate the propagation from the condenser lens (L_c) to the Ti:sapphire image plane as shown in Fig. 2, the two-step propagation in Eq. (8) [22] is used. t_{LA2} and t_c are the transmittance function of LA2 and condenser lens, respectively. Because d_{2c} is set to 0, both t_{LA2} and t_c must be applied to the equation. L_1 and L_2 are the plane sizes of LA2 and Ti:sapphire for the

Optics EXPRESS

simulation, respectively. x_1, y_1 and x_2, y_2 are the coordinates of the plane of LA2 and the image plane. f_{X1}, f_{Y1} are the frequency coordinates of the plane of LA2.

$$E_{crystal}(x_2, y_2) = \frac{L_2}{L_1} exp(jkd_{ci}) exp\Big[-j\frac{k}{2d_{ci}}\frac{L_1 - L_2}{L_2}(x_2^2 + y_2^2)\Big] \times F^{-1}\Big\{exp\Big[-j\pi\lambda d_{ci}\frac{L_1}{L_2}(f_{X1}^2 + f_{Y1}^2)\Big] F\Big\{U_1(x_1, y_1) exp\Big[j\frac{k}{2d_{ci}}\frac{L_1 - L_2}{L_2}(x_1^2 + y_1^2)\Big]\Big\}\Big\}, \quad (8)$$

$$U_1(x, y) = E_{LA2}(x, y) t_{LA2}(x, y) t_c(x, y), \quad (9)$$

$$t_{LA2}(x, y) = \sum_n \Big[rect\Big(\frac{x - \Delta x_n}{p}\Big) rect\Big(\frac{y - \Delta y_n}{p}\Big) exp\Big[-j\frac{k}{2f_2}\{(x-\Delta x_n)^2 + (y-\Delta y_n)^2\}\Big]\Big], \quad (10)$$

$$t_c(x, y) = exp\Big[-j\frac{k}{2f_c}(x^2 + y^2)\Big], \quad (11)$$

There is an interference on the image plane when using the beam homogenizer [16]. There has also been concern about the interference effect because a general petawatt amplifier uses several pump beams to provide a sufficient energy [20, 23]. However, previous experimental results show that the interference does not have a significant effect on the output beam and not damage a surface of the gain medium [20, 23]. In the setup of a general Ti:sapphire amplifier, the input beam passes through the crystal several times with a tilted angle, and the pump beam enters the crystal at a tilted angle. Because the input beam energy is integrated with the propagation direction, it will blur a Talbot effect. The interference effect also will be eliminated by this structure. A detailed investigation will be conducted in a further study. In this research, we will ignore the interference effect on the image plane for amplification simulation.

3. Optimization of the beam homogenizer

3.1. Design of beam homogenizer for high steepness

The steepness of the pump beam is defined as edge steepness in Eq. (12) according to ISO standard [24]. $A_{10\%}, A_{90\%}$ are irradiation areas with energy density values above 10% and 90% of maximum energy density, respectively. However, maximum energy density does not assure reliability of the result because local hot spot influences it significantly [25]. For this reason, we use peak energy density in the histogram curve instead of maximum energy density as proposed by ENEA [25]. It is important to design the beam homogenizer with a high steepness because the higher the steepness, the more energy is transferred to the input beam [14, 20].

$$S_{10\%,90\%} = \frac{A_{10\%} - A_{90\%}}{A_{10\%}}, \quad (12)$$

In the geometric optical imaging condition($d_{12} = f_2$), a high steepness of the edge is guaranteed without considering a diffraction effect. Since an image of where the incident beam is divided by LA1 is formed on the image plane, a sharp edge is obtained at the center of the Ti:sapphire crystal [21]. The edge steepness by the lens pitch is shown in Fig. 3. A larger lens pitch decreases the diffraction effect; therefore, the edge of the pump beam has a high steepness. If the lens pitch is lower, the steepness of the edge decreases by the diffraction effect.

Optics EXPRESS

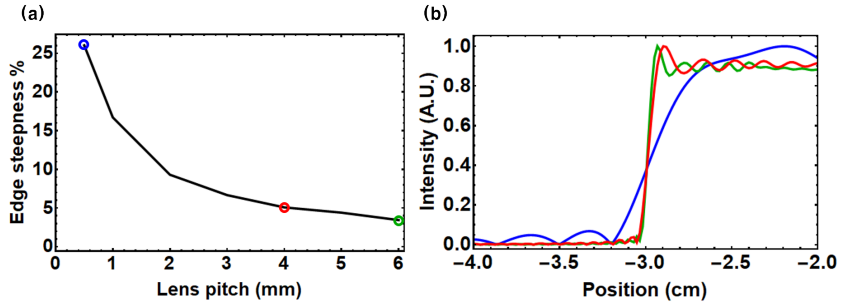

Fig. 3. Relation between lens pitch and edge steepness: (a) lens pitch vs. edge steepness, and (b) position vs. intensity. Lens pitch is 0.5 (blue), 4.0 (red), and 6.0 *mm* (green), respectively.

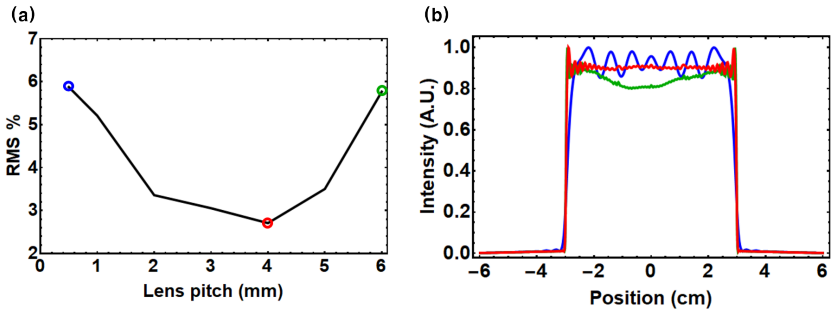

Fig. 4. Relation between lens pitch and RMS uniformity: (a) lens pitch vs. RMS uniformity, and (b) position vs. intensity. Lens pitch is 0.5 (blue), 4.0 (red), and 6.0 *mm* (green), respectively.

3.2. *Design of beam homogenizer for uniform spatial distribution*

The spatial uniformity of the pump beam is defined as the normalized root mean square (RMS) in Eq. (13) according to the ISO standard definition [24]. $H_{\eta ave}$ and A_{η}^{i} are a spatially averaged energy density and irradiation area above η of peak energy density H_{peak} is proposed by [25] for reliability of the result, not maximum energy density, respectively. The uniform spatial distribution of the pump beam is important in obtaining a uniform spatial distribution of the output beam [14]. Because of the high gain of the amplifier, the amplified beam has almost the same spatial distribution as the pump beam.

$$U_{\eta} = \frac{1}{H_{\eta ave}} \sqrt{\frac{1}{A_{\eta}^{i}} \iint [H(x,y) - H_{\eta ave}]^2 dxdy}, \tag{13}$$

Figure 4 shows the RMS value of the spatial uniformity $U_{0.9}$ of the output beam by the lens pitch. An RMS spatial uniformity of 2.7% is achieved when the lens pitch is 4 *mm*. When the lens pitch is less than 4 *mm*, the RMS spatial uniformity increases by the diffraction effect by the small lens pitch. When the lens pitch is more than 4 *mm*, the RMS spatial uniformity gets worse because the number of beamlets in the lens array is not enough to remove the effect of the nonuniform input beam and separated beamlets. As a countermeasure to this problem, a freeform microlens array homogenizer was recently proposed [26]. This system showed excellent performance in uniformity and steepness. However, the input beam profile influences the performance because the optimization process was based on the spatial distribution of the input beam.

Optics EXPRESS

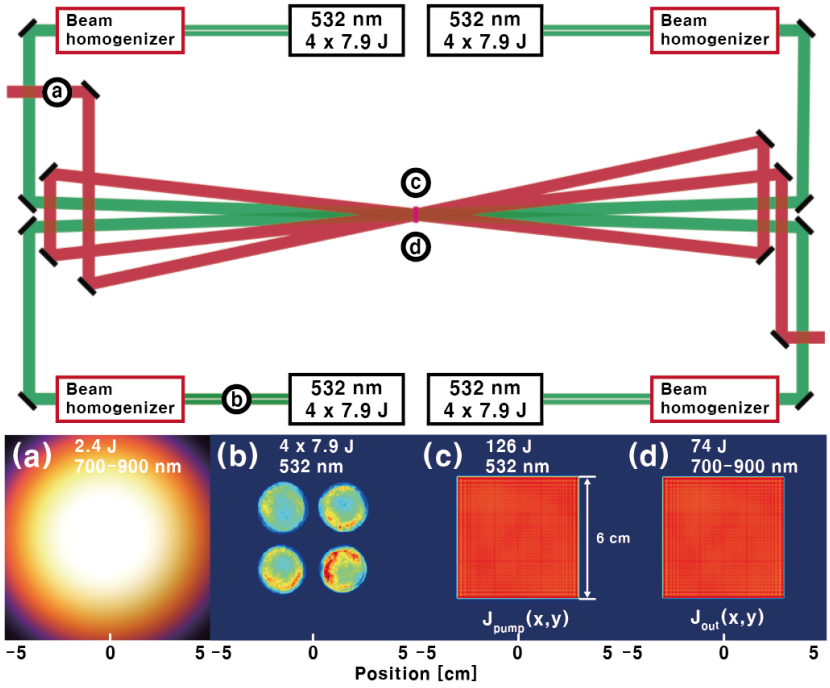

Fig. 5. The structure of Ti:sapphire amplifier: (a) input beam, (b) nonuniform pump beam, (c) shaped pump beam by beam homogenizer, and (d) amplified beam (output).

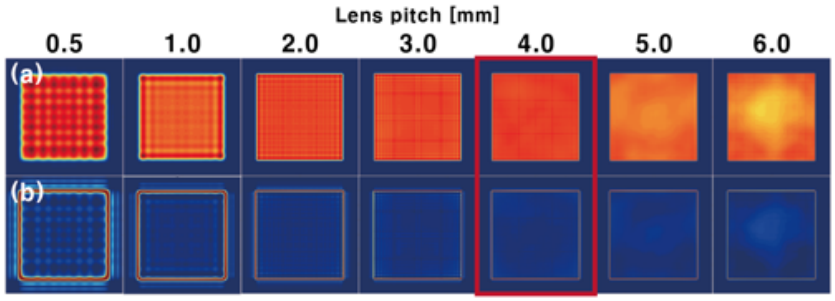

Fig. 6. Amplification simulation with various conditions: (a) output beam and (b) residual pump beam. Red box indicates optimum result.

3.3. 2D amplification simulation

The designed beam homogenizer generates a uniform square pump beam, which is used for a 2D amplification simulation using the Frantz-Nodvik equation in Eqs. (14) and (15) [27]. J_{in}, J_{out}, and $J_{sat} = h\nu/\sigma$ are the input fluence, the output fluence, and the saturation fluence, respectively. J_{pump} is the fluence of two dimensional electric field calculated from Eq. (8).

$$J_{out}(x,y) = J_{sat} ln\Big[1 + G_0(x,y)\Big(exp\Big[\frac{J_{in}(x,y)}{J_{sat}}\Big] - 1\Big)\Big], \tag{14}$$

$$G_0(x,y) = exp[\lambda_{pump}/\lambda_{laser} \cdot J_{pump}(x,y)/J_{sat}], \tag{15}$$

Optics EXPRESS

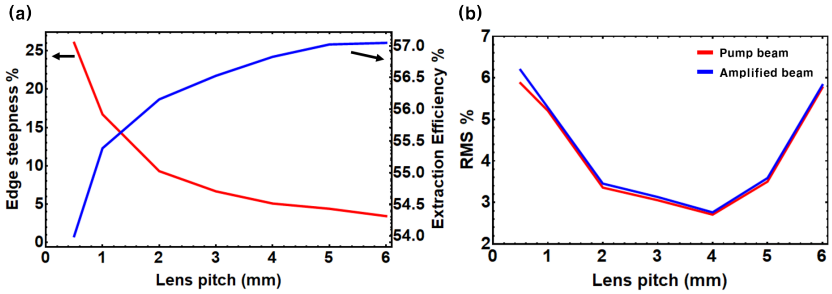

Fig. 7. Influence of pump beam on output beam: (a) edge steepness of pump beam (red) vs. extraction efficiency (blue), and (b) RMS spatial uniformity of pump beam (red) and output beam (blue) according to lens pitch.

Figure 5 illustrates the structure of a Ti:sapphire amplifier. The chirped input beam by an öffner stretcher [28] has 2.4 J of energy and 700–900 *nm* of bandwidth. Sixteen nonuniform pump beams enter into four beam homogenizers and form a square-shaped flat-top beam of width 6 *cm* and 126 J of energy on a Ti:sapphire crystal. The input beam passes through the gain medium three times. The spatial distribution of the output beam is almost the same as the spatial distribution of the pump beam.

Figure 6 shows a 2D image of the intensity of the output beam and the residual pump beam. When the lens pitch is small, the spatial distribution of the output beam is nonuniform owing to the poor spatial uniformity of the pump beam. There is residual pump beam at the edge because of the low steepness of the pump beam. When the lens pitch is large, there is little residual pump beam by the high steepness of the pump beam. However, the spatial uniformity of the output beam is nonuniform because of the poor spatial uniformity of the pump beam. When the lens pitch is 4 *mm*, the spatial uniformity of the output beam is uniform, and there is almost no residual pump energy by high steepness.

Figure 7(a) shows the influence of the edge steepness of the pump beam on the extraction efficiency. Since the edge steepness is higher, the extraction efficiency is higher. If the edge steepness is low, the edge of the beam cannot extract the pump energy because of low pumping fluence.

Figure 7(b) shows that the spatial distribution of the output beam follows the spatial distribution of the pump beam. It turns out that a low RMS of the pump beam leads to a low spatial uniformity of the output beam.

The extraction efficiency is higher than 54% regardless of the size of the lens pitch. In a practical Ti:sapphire laser amplifier, the extraction efficiency is usually between 40 – 50% [20,23]. The existing system shows super-gaussian order about 10 to 20, but pump beam shaped by imaging beam homogenizer like we introduced shows super-gaussian order more than 100. Because most of residual pump energy comes from the edge of the beam, so high steepness pump beam improves the extraction efficiency. But there will be additional efficiency loss in practice by parasitic lasing not considered in simulation.

The optimal pitch size for pumping amplifier is 4 *mm* when the spatial uniformity is lowest. The extraction efficiency is 56.8% with $1.2cm^{-1}$ of the absorption coefficient and residual pump energy is only 3.7 J, which means most of the pump energy is extracted with 97% of efficiency. The RMS value of the spatial uniformity of the output beam is 2.7%, which is the lowest value in this simulation. The output beam has 74 J of energy when 120 J of energy is stored in the crystal. The extraction efficiency is close to the quantum defect efficiency, which is the ratio between the wavelength of the pump beam(532 *nm*) and the wavelength of the seed beam (700–900 *nm*) [29].

Optics EXPRESS

4. Conclusion

We have designed a square-shaped beam homogenizer with high steepness and uniformity for a petawatt-class Ti:sapphire amplifier. The beam homogenizer exhibited its best pumping performance when the lens pitch was 4 *mm*. The designed beam homogenizer generated a pump beam with 5.1% of edge steepness and 2.7% of RMS spatial uniformity. The results of a 2D amplification simulation with the designed beam were obtained an extraction efficiency of 56.8%, an edge steepness of 4.2% and a RMS spatial uniformity of 2.7% for the output beam. In addition, 74 J of output energy was achieved. By this result, we should obtain more than 2 PW of peak power when the efficiency of the pulse compressor is considered [20]. By these results, it is shown that the beam homogenizer using lens arrays is effective for improving an efficiency of the amplifier and reducing the size of the petawatt laser system.

Funding

Ministry of Trade, Industry & Energy (MI, Korea) (10048964).